Inorganica Chimica Acta, 195 (1992) 25–33

Transition metal complexes with sulfur ligands LXXXVII*. Coordination of CO to high valent molybdenum sulfur centers: syntheses, properties and structure of stable molybdenum(IV) thiolato carbonyl complexes

Dieter Sellmann**, Franz Grasser, Falk Knoch and Matthias Moll
Institut für Anorganische Chemie der Universität Erlangen-Nürnberg, Egerlandstrasse 1, W-8520 Erlangen (FRG)

(Received December 12, 1991)

Abstract

Thermal thioether-*S*-desalkylation of the molybdenum(II) carbonyl complexes [Mo(CO)$_2$(PR$_3$)(‘^{bu}S$_4$’)] (R = Ph, Me; ‘^{bu}S$_4$’$^{2-}$ = 1,2-bis(2-mercapto-3,5-di-t-butylphenylthio)ethane(2 −)) yields the molybdenum(IV) carbonyl complexes [Mo(CO)(PR$_3$)(‘^{bu}S$_2$’)$_2$] (‘^{bu}S$_2$’$^{2-}$ = 3,5-di-t-butyl-1,2-benzenedithiolate(2 −)). X-ray structure analysis of [Mo(CO)(PPh$_3$)(‘^{bu}S$_2$’)$_2$] (**1**) shows a pseudo trigonal prismatic coordination of the molybdenum center by a S$_4$CP donor set. NMR spectra indicate that **1** and [Mo(CO)(PMe$_3$)(‘^{bu}S$_2$’)$_2$] (**2**) possess *trans* octahedral structures in solution. Thermal desalkylation of [Mo(CO)$_3$(‘^{bu}S$_4$’)] at room temperature in high *vacuo* yields [Mo(CO)$_2$(‘^{bu}S$_2$’)$_2$] (**4**), the first molybdenum(IV) carbonyl complex displaying only biologically relevant thiolate donors in its coordination sphere and being stable at room temperature.

Introduction

The active sites of most nitrogenases contain iron, molybdenum and sulfur donors [2]. Even after the discovery of ‘Fe-only’ nitrogenases [3], it cannot absolutely be excluded that in Fe/Mo nitrogenases the molybdenum centers are the binding sites of the nitrogenase substrates. In addition to N$_2$ these are in particular C$_2$H$_2$ and the strong nitrogenase inhibitor CO. It must be noted, however, that this function of molybdenum has never been proved though it was often postulated or tacitly taken for granted [4]. According to numerous investigations the molybdenum centers in nitrogenases exhibit oxidation states of +IV or even higher [5]. Therefore a number of efforts was made to obtain high valent molybdenum sulfur complexes that bind N$_2$ or the isoelectronic CO in order to serve as model compounds and to prove the supposed role of molybdenum [6].

Carbon monoxide, however, usually binds to metal centers in low oxidation states and only a very few high-valent molybdenum carbonyl complexes are known. These are, for example, *trans*-[Mo(O)$_2$(CO)$_4$] that is labile and only observable at 20 K as intermediate in the photo oxidation of [Mo(CO)$_6$] in an argon matrix [7], or the thermally more stable [(η^5-C$_5$H$_5$)Mo(CO)$_2$(X)$_3$] (X = Cl, Br, I) [8a, b] and [(η^5-CH$_3$C$_5$H$_4$)Mo(CO)$_2$(I)$_3$] [8c] complexes. While the molybdenum centers of these complexes carry no biologically relevant thiolate coligands, such thiolate donors are found in [Mo(CO)(PMePh$_2$)(‘S$_2$’)$_2$] (‘S$_2$’$^{2-}$ = 1,2-benzenedithiolate(2 −)), but here again the coordination of CO is so labile that the complex can be isolated only in an atmosphere of CO gas [9].

We have now observed the formation of molybdenum(IV) thiolate carbonyl complexes that are thermally stable and could be fully characterized, in one case even by X-ray structure analysis. Preliminary results were published elsewhere [1b].

Experimental

General

Unless otherwise noted all synthetic procedures were carried out under nitrogen atmosphere at room temperature by using standard Schlenk techniques. Solvents were dried and distilled before use. As far as possible the reactions were monitored by IR or NMR spectroscopy. Spectra were recorded on the following instruments: IR (CaF$_2$ cuvettes or KBr discs): Zeiss IMR 25, Perkin-Elmer 983 or Perkin-Elmer 1620 FT IR; solvent bands were compensated. NMR: JEOL

---

*For Part LXXXVI see ref. 1a.

**Author to whom correspondence should be addressed.

0020-1693/92/$5.00

FT-JNM-GX 270 and EX 270. Mass spectra: Varian MAT 212. [Mo(CO)$_2$(PPh$_3$)(‘^{bu}S$_4$’)] [10], [Mo(CO)$_2$(PMe$_3$)(‘^{bu}S$_4$’)] [10] and [Mo(CO)$_3$(‘^{bu}S$_4$’)] [10] were prepared by literature methods.

Syntheses

[Mo(CO)(PPh$_3$)(‘^{bu}S$_2$’)$_2$] (1)

The orange coloured solution of [Mo(CO)$_2$(PPh$_3$)(‘^{bu}S$_4$’)] (950 mg, 1.0 mmol) in 35 ml of THF was heated for 75 min under reflux. The colour of the reaction mixture rapidly turned deep red. The solution was evaporated to dryness yielding a violet–red residue which was dried *in vacuo* for 12 h and redissolved in 10 ml of CH$_2$Cl$_2$. The solution was filtered through a layer of SiO$_2$ (5 cm) and the filtrate was evaporated to dryness, yielding a deep red residue which was recrystallized from 25 ml of CH$_2$Cl$_2$/MeOH (1:1.5) (+20 → −30 °C). The precipitated dark red microcrystals were separated, washed with 50 ml of MeOH and 16 ml of n-hexane, and dried *in vacuo*. Yield 390 mg (44%).

Anal. Calc. for C$_{47}$H$_{55}$OPS$_4$Mo (891.1) = [Mo(CO)(PPh$_3$)(‘^{bu}S$_2$’)$_2$]: C, 63.35; H, 6.22; S, 14.39. Found: C, 63.22; H, 6.47; S, 14.11%.

IR (KBr): ν(CO) = 1978 cm^{-1}. NMR (CDCl$_3$, δ (ppm)): ^{1}H NMR (270 MHz): 8.16 (d, 2H, C$_6$*H*$_2$); 8.0–6.9 (broad, 12H, P(C$_6$*H*$_5$)$_3$, superimposed); 7.45 (d, 2H, C$_6$*H*$_2$, superimposed); 6.9–6.3 (broad, 3H, P(C$_6$*H*$_5$)$_3$); 1.61 (s, 18H, C$_4$*H*$_9$); 1.36 (s, 18H, C$_4$*H*$_9$). ^{31}P{^{1}H} NMR (109.38 MHz): 55.56 (s, *P*Ph$_3$). ^{13}C{^{1}H} NMR (67.94 MHz): 231.73 (d, *C*O, $^{2}J(^{31}\mathrm{P}^{13}\mathrm{C}) = 11.5$ Hz), 159.39, 152.05, 148.72, 147.63, 135.30 (d, $^{2}J(^{31}\mathrm{P}^{13}\mathrm{C}) = 8.6$ Hz), 130.95, 129.06, 128.91, 125.10, 120.83 (C_{aryl}); 38.08, 35.43, 32.17, 31.21 (C_{alkyl}). FD mass spectrum (CS$_2$, ^{98}Mo (*m*/*z*)): 892 ([Mo(CO)(PPh$_3$)(‘^{bu}S$_2$’)$_2$]$^+$).

[Mo(CO)(PMe$_3$)(‘^{bu}S$_2$’)$_2$] (2) and [Mo(PMe$_3$)$_2$(‘^{bu}S$_2$’)$_2$] (3)

The orange coloured solution of [Mo(CO)$_2$(PMe$_3$)(‘^{bu}S$_4$’)] (550 mg, 0.72 mmol) in 50 ml of THF was refluxed for 2.5 h while CO was slowly bubbled through the solution. The colour of the reaction mixture rapidly turned deep red. The solution was evaporated to dryness yielding a deep red residue which was dissolved in 20 ml of CH$_2$Cl$_2$. The solution was filtered through a layer of SiO$_2$ (*c.* 10 g) and the SiO$_2$ was washed with about 60 ml of CH$_2$Cl$_2$ until only black–green residues remained adsorbed at the SiO$_2$. The combined filtrates were evaporated to dryness, and the residue was dissolved in CH$_2$Cl$_2$ at 35 °C. A fourfold amount of MeOH was added, and the mixture was cooled to −30 °C. Orange microcrystals of the byproduct **3** precipitated, which were separated and washed with 80 ml of MeOH.

The deep red mother liquor was combined with the 80 ml of MeOH used for washing, and the solution was evaporated to dryness. The red residue was dissolved in n-pentane and purified by chromatography (SiO$_2$:ICN Silica 100–200 60A; column: $l = 13$ cm, $d = 3.5$ cm). Small amounts of a CO free green species were eluted by n-pentane. Subsequent elution of the column with n-pentane/CH$_2$Cl$_2$ (9:1) yielded a deep red powder of **2**. Yield 300 mg (59%).

Anal. Calc. for C$_{32}$H$_{49}$OPS$_4$Mo (704.9) = [Mo(CO)(PMe$_3$)(‘^{bu}S$_2$’)$_2$]: C, 54.52; H, 7.01; S, 18.20. Found: C, 54.21; H, 7.22; S, 18.21%.

IR (KBr): ν(CO) = 1968 cm^{-1}; δ_{PCH} = 949 cm^{-1}. NMR (CDCl$_3$, δ (ppm)): ^{1}H NMR (270 MHz): 8.25 (d, 2H, C$_6$*H*$_2$); 7.53 (d, 2H, C$_6$*H*$_2$); 1.79 (s, 18H, C$_4$*H*$_9$); 1.64 (d, 9H, P(C*H*$_3$)$_3$); 1.42 (s, 18H, C$_4$*H*$_9$). ^{31}P{^{1}H} NMR (109.38 MHz): 22.97 (s, *P*Me$_3$). ^{13}C{^{1}H} NMR (67.94 MHz): 233.62 (d, *C*O, $^{2}J(^{31}\mathrm{P}^{13}\mathrm{C}) = 10.3$ Hz); 159.09 (d, $J(^{31}\mathrm{P}^{13}\mathrm{C}) = 2.7$ Hz), 151.77, 148.69, 147.81, 125.02 (d, $J(^{31}\mathrm{P}^{13}\mathrm{C}) = 7.9$ Hz), 120.91 (C_{aryl}); 38.20, 35.43, 32.17, 31.26, 20.55 (d, $^{1}J(^{31}\mathrm{P}^{13}\mathrm{C}) = 32.6$ Hz) (C_{alkyl}). FD mass spectrum (CS$_2$, ^{98}Mo (*m*/*z*)): 706 ([Mo(CO)(PMe$_3$)(‘^{bu}S$_2$’)$_2$]$^+$).

The byproduct **3** was washed with 50 ml of n-pentane and dissolved in 7.5 ml of CH$_2$Cl$_2$. The solution was layered with 15 ml of MeOH and stored at room temperature for 14 days. Orange needles of **3** precipitated, were separated, washed with MeOH and n-pentane, and dried *in vacuo*. Yield 120 mg (22%).

Anal. Calc. for C$_{34}$H$_{58}$P$_2$S$_4$Mo (753.0) = [Mo(PMe$_3$)$_2$(‘^{bu}S$_2$’)$_2$]: C, 54.23; H, 7.76; S, 17.03. Found: C, 54.19; H, 8.15; S, 16.74%.

IR (KBr): δ_{PCH} = 952 cm^{-1}. NMR (CDCl$_3$, δ (ppm)): ^{1}H NMR (270 MHz): 8.13 (d, 2H, C$_6$*H*$_2$); 7.39 (d, 2H, C$_6$*H*$_2$); 1.77 (d, 18H, P(C*H*$_3$)$_3$, superimposed); 1.75 (s, 18H, C$_4$*H*$_9$, superimposed); 1.38 (s, 18H, C$_4$*H*$_9$). ^{31}P{^{1}H} NMR (109.38 MHz): 14.82 (s, *P*Me$_3$). ^{13}C{^{1}H} NMR (67.94 MHz): 157.32, 149.75, 147.53, 146.27, 124.42, 119.62 (C_{aryl}); 38.08, 35.28, 32.32, 31.21, 22.48 (d, $^{1}J(^{31}\mathrm{P}^{13}\mathrm{C}) = 30.9$ Hz) (C_{alkyl}). FD mass spectrum (CH$_2$Cl$_2$, ^{98}Mo (*m*/*z*)): 754 ([Mo(PMe$_3$)$_2$(‘^{bu}S$_2$’)$_2$]$^+$).

[Mo(CO)$_2$(‘^{bu}S$_2$’)$_2$] (4)

When solid orange–red [Mo(CO)$_3$(‘^{bu}S$_4$’)] (100 mg, 0.14 mmol) was kept in a Schlenk tube at room temperature in high *vacuo*, the vacuum being maintained by continuous pumping, it slowly decomposed in the course of 15 days. The reaction was monitored by IR spectroscopy; within regular periods of *c.* 24 h, probes were taken which were dissolved in n-pentane. After 15 days, the resulting deep violet solid was dissolved in n-pentane/CH$_2$Cl$_2$ (19:1) and purified by chromatography at 15 °C (SiO$_2$: ICN Silica 100–200 60A;

column: $l = 13$ cm, $d = 3.5$ cm). With n-pentane/CH_2Cl_2 (19:1) a blue–violet zone was eluted that yielded solid bright blue–violet **4**. Because of its electrostatic charge it could not be characterized by elemental analysis but only by IR, NMR and FD mass spectroscopy. Yield 55 mg (60%).

IR (KBr): $\nu(CO) = 2035, 1997\ cm^{-1}$. NMR ($CDCl_3$, δ (ppm)): ^1H NMR (270 MHz): 8.30 (d, 2H, C_6H_2); 7.64 (d, 2H, C_6H_2); 1.77 (s, 18H, C_4H_9); 1.42 (s, 18H, C_4H_9). $^{13}C\{^1H\}$ NMR (67.94 MHz): 222.04 (CO); 160.84, 153.26, 149.67 (2 signals superimposed), 125.63, 122.47 (C_{aryl}); 38.39, 35.61, 32.02, 31.24 (C_{alkyl}). FD mass spectrum (CS_2, ^{98}Mo (m/z)): 658 ($[Mo(CO)_2(\text{‘}^{bu}S_2\text{’})_2]^+$).

X-ray structure analysis of [Mo(CO)(PPh$_3$)(‘^{bu}S$_2$’)$_2$] (1)

Single crystals of **1** were obtained by cooling a saturated CH_2Cl_2/MeOH (1:1) solution from 35 °C to room temperature. A single crystal was sealed under N_2 in a glass capillary. The structure was solved by direct methods. Non-hydrogen atoms were refined anisotropically and the aromatic H atoms were placed at calculated positions and refined as rigid groups. The H atoms of the methyl groups were placed in ideal tetrahedron positions and rotated around their central C atom during refinement. H atoms were refined with common isotropic temperature factors. Table 1 summarizes crystallographic data for **1**, the fractional atomic coordinates are listed in Table 2. See also ‘Supplementary material’.

TABLE 1. Selected crystallographic data of **1**

Formula	$C_{46}H_{55}MoOPS_4$
Molecular weight	891.13
Space group	$P2_12_12_1$
Crystal system	orthorhombic
Crystal size (mm)	0.40×0.30×0.10
Cell dimensions	
a (pm)	1446.7(9)
b (pm)	1645.8(7)
c (pm)	1922.2(10)
V (pm^3)	$4577(4)\times10^6$
Z	4
D_{calc} (g/cm^3)	1.29
μ (cm^{-1})	5.2
Radiation (pm)	Mo Kα; 71.073
Diffractometer	Nicolet R3m/V
Scan technique	ω-scan
Scan speed (°/min)	3.0–15
2θ Range (°)	$3<2\theta<54$
Reflections measured	9342
Independent reflections	8881
Observed reflections	7421
σ-Criterion	$F>4\sigma(F)$
Temperature of measurement (K)	200
Absorption correction	none
Program	SHELXTL PLUS
R; R_w (%)	6.2; 4.7
Weight	$1/\sigma^2$
Parameters refined	488

Results and discussion

Syntheses and reactions

When the NMR spectra of the $[Mo(CO)_2(PR_3)(\text{‘}^{bu}S_4\text{’})]$ (R = Ph, Me) complexes [10] were recorded at room temperature it was observed that the dicarbonyl complexes are thermally labile and slowly decompose. All decomposition products could be identified by their ^1H, $^{13}C\{^1H\}$ and $^{31}P\{^1H\}$ NMR signals such that conclusions could be drawn which reactions took place in solution. $[Mo(CO)_2(PPh_3)(\text{‘}^{bu}S_4\text{’})]$, for example, splits off C_2H_4 by thioether-S-desalkylation of the ‘$^{bu}S_4$’ ligand, loses also one CO ligand, and gives $[Mo(CO)(PPh_3)(\text{‘}^{bu}S_2\text{’})_2]$ (**1**) according to eqn. (1).

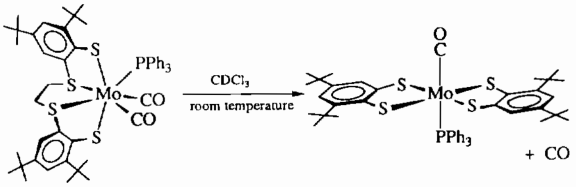

(1)

$[Mo(CO)_2(PPh_3)(\text{‘}^{bu}S_4\text{’})]$ $[Mo(CO)(PPh_3)(\text{‘}^{bu}S_2\text{’})_2]$

1

1, in solution, has a *trans*-octahedral structure as indicated in eqn. (1), in solid state, however, it exhibits a trigonal prismatic coordination geometry (see below).

The released CO substitutes the PPh_3 ligand of still unreacted $[Mo(CO)_2(PPh_3)(\text{‘}^{bu}S_4\text{’})]$ that is converted into $[Mo(CO)_3(\text{‘}^{bu}S_4\text{’})]$ according to eqn. (2).

$$[Mo(CO)_2(PPh_3)(\text{‘}^{bu}S_4\text{’})] + CO \xrightarrow[\text{room temperature}]{CDCl_3} [Mo(CO)_3(\text{‘}^{bu}S_4\text{’})] + PPh_3 \quad (2)$$

Formation of $[Mo(CO)_3(\text{‘}^{bu}S_4\text{’})]$ in solutions of $[Mo(CO)_2(PPh_3)(\text{‘}^{bu}S_4\text{’})]$ at room temperature can also be observed by IR spectroscopy. The PMe_3 derivative $[Mo(CO)_2(PMe_3)(\text{‘}^{bu}S_4\text{’})]$ also eliminates CO and C_2H_4 and transforms into $[Mo(CO)(PMe_3)(\text{‘}^{bu}S_2\text{’})_2]$ (**2**) (eqn. (3)).

$$[Mo(CO)_2(PMe_3)(\text{‘}^{bu}S_4\text{’})] \xrightarrow[\text{room temperature}]{CDCl_3} \underset{\mathbf{2}}{[Mo(CO)(PMe_3)(\text{‘}^{bu}S_2\text{’})_2]} + CO + C_2H_4 \quad (3)$$

This reaction, however, is slower than the reaction according to eqn. (1), and no substitution of PMe_3 in $[Mo(CO)_2(PMe_3)(\text{‘}^{bu}S_4\text{’})]$ by released CO takes place. Formation of C_2H_4 in reactions (1) and (3) was indicated by the ^1H NMR C_2H_4 singlet at 5.25 ppm (in CS_2).

TABLE 2. Fractional atomic coordinates ($\times 10^2$) and isotropic thermal parameters ($pm^2 \times 10^{-1}$) of the non-hydrogen atoms of **1**

	x	y	z	U_{eq}[a]
Mo(1)	2188(1)	9401(1)	7120(1)	23(1)
C(1)	2930(5)	8458(3)	7527(3)	35(2)
O(1)	3342(3)	7929(3)	7742(2)	54(2)
S(1)	3700(1)	9784(1)	6819(1)	29(1)
S(2)	2070(1)	10803(1)	7355(1)	27(1)
S(3)	638(1)	9469(1)	6736(1)	27(1)
S(4)	2296(1)	8555(1)	6138(1)	31(1)
C(15)	3007(4)	11285(3)	6969(2)	25(2)
C(14)	2966(4)	12138(3)	6877(3)	29(2)
C(13)	3678(5)	12532(3)	6547(3)	29(2)
C(12)	4449(4)	12079(3)	6332(3)	29(2)
C(11)	4536(4)	11248(3)	6412(3)	28(2)
C(10)	3777(4)	10833(3)	6735(3)	25(2)
C(110)	5417(4)	10804(3)	6151(3)	32(2)
C(111)	5161(5)	10203(3)	5561(3)	40(2)
C(112)	5899(4)	10354(4)	6767(3)	45(2)
C(113)	6130(4)	11404(4)	5845(3)	48(2)
C(130)	3655(5)	13443(3)	6379(3)	39(2)
C(131)	2866(6)	13873(4)	6724(4)	02(4)
C(132)	3597(8)	13572(5)	5617(3)	29(6)
C(133)	4510(6)	13848(4)	6662(5)	06(5)
C(25)	1268(4)	8546(3)	5679(3)	24(2)
C(24)	1247(5)	8167(3)	5028(3)	30(2)
C(23)	451(5)	8181(3)	4640(3)	29(2)
C(22)	−341(4)	8550(3)	4927(3)	30(2)
C(21)	−368(4)	8911(3)	5573(3)	29(2)
C(20)	484(4)	8940(3)	5958(3)	24(2)
C(210)	1287(4)	9243(4)	5864(3)	37(2)
C(211)	1233(5)	10169(4)	6022(3)	54(3)
C(212)	2084(4)	9127(4)	5336(3)	51(2)
C(213)	1532(5)	8761(4)	6532(3)	57(3)
C(230)	401(5)	7820(4)	3902(3)	35(2)
C(231)	100(6)	8476(4)	3384(3)	67(3)
C(232)	1341(5)	7520(5)	3651(3)	71(3)
C(233)	−272(6)	7115(4)	3902(4)	79(4)
P(1)	1352(1)	9296(1)	8264(1)	27(1)
C(35)	25(5)	8305(4)	8910(3)	42(2)
C(34)	−476(5)	7583(4)	8989(3)	42(2)
C(33)	−368(6)	6954(4)	8530(3)	51(3)
C(32)	239(5)	7029(4)	7975(3)	51(3)
C(31)	756(5)	7729(3)	7890(3)	40(2)
C(30)	660(4)	8376(3)	8354(3)	29(2)
C(45)	2032(5)	8779(4)	9576(3)	41(2)
C(44)	2652(5)	8813(4)	10125(3)	49(3)
C(43)	3416(5)	9307(4)	10094(3)	50(3)
C(42)	3588(5)	9762(4)	9517(3)	48(2)
C(41)	2962(5)	9743(3)	8956(3)	41(2)
C(40)	2179(5)	9260(3)	8988(2)	29(2)
C(55)	849(5)	10768(3)	8909(3)	47(2)
C(54)	216(7)	11381(4)	9082(4)	63(3)
C(53)	−684(7)	11332(5)	8868(4)	67(4)
C(52)	−992(5)	10690(4)	8475(3)	55(3)
C(51)	−375(5)	10082(4)	8293(3)	41(2)
C(50)	546(5)	10100(3)	8513(3)	32(2)

[a] Equivalent isotropic U defined as one third of the trace of the orthogonalized U_{ij} tensor.

The thermal decomposition of $[Mo(CO)_2(PPh_3)(\text{‘}^{bu}S_4\text{’})]$ (eqn. (1)) also allowed the direct synthesis of the molybdenum(IV) carbonyl complex **1** according to eqn. (4).

$$[Mo(CO)_2(PPh_3)(\text{‘}^{bu}S_4\text{’})] \xrightarrow[\text{75 min}]{\text{THF/65 °C}}$$
$$1 + CO + C_2H_4 + \text{other products} \qquad (4)$$

Already when warmed up the reaction mixture changes colour from orange to deep red. In the solution IR spectra, the ν(CO) bands of the educt (1943, 1882 cm^{-1}) finally disappear while the intense ν(CO) absorption of **1** at 1978 cm^{-1} increases (Fig. 1). (The weak ν(CO) band at 1899 cm^{-1} is due to a byproduct that has not yet been characterized.) Isolated dark red **1** is well soluble in CS_2, CH_2Cl_2, $CHCl_3$, THF and acetone.

2 was synthesized by an analogous procedure (eqn. (5)) but CO gas had to be bubbled through the boiling reaction solution in order to suppress formation of the byproduct $[Mo(PMe_3)_2(\text{‘}^{bu}S_2\text{’})_2]$ (**3**).

$$[Mo(CO)_2(PMe_3)(\text{‘}^{bu}S_4\text{’})] \xrightarrow[\text{2.5 h}]{\text{+CO/THF/65 °C}}$$
$$2 + CO + C_2H_4 + [Mo(PMe_3)_2(\text{‘}^{bu}S_2\text{’})_2] \qquad (5)$$

The dark red **2** is well soluble in all common organic solvents and shows a characteristic ν(CO) band at 1968 cm^{-1} in the KBr IR spectrum.

The orange–brown byproduct **3** is well soluble in CS_2, CH_2Cl_2, $CHCl_3$, acetone and THF and sparingly soluble in MeOH, n-hexane and Et_2O. Its KBr IR spectrum exhibits an intense δ_{PCH} band at 952 cm^{-1} in addition to the characteristic absorptions of the ‘$^{bu}S_2$’ ligands.

If the thermal decomposition of $[Mo(CO)_2(PMe_3)(\text{‘}^{bu}S_4\text{’})]$ is carried out without simultaneous bubbling of CO gas through the reaction mixture

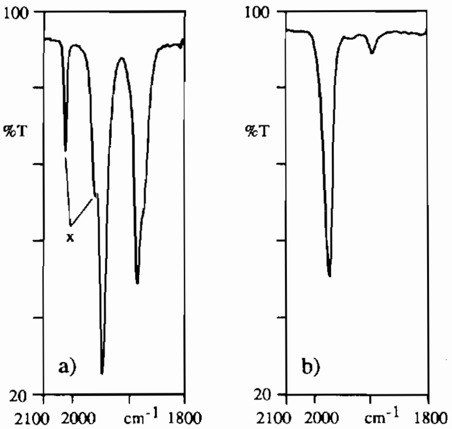

Fig. 1. ν(CO) IR spectrum of the THF solution of: (a) $[Mo(CO)_2(PPh_3)(\text{‘}^{bu}S_4\text{’})]$ at 20 °C (x = $[Mo(CO)_3(\text{‘}^{bu}S_4\text{’})]$) and (b) after 75 min. at 65 °C.

the major product is indeed **2** but the amount of the byproduct is considerably higher.

One PMe_3 ligand of **3** is labile and can easily be substituted by CO according to eqn. (6).

$$3 \xrightarrow[3.5\ h]{+CO/THF/20\ °C} 2 + PMe_3 \qquad (6)$$

This reaction is conveniently monitored by IR spectroscopy. When CO is bubbled through the THF solution of **3**, it slowly changes colour from orange–brown to deep red, and the intense ν(CO) absorption of **2** appears at 1966 cm^{-1}. This reaction also explains why formation of **3** in reaction (5) can be suppressed by additional CO.

With respect to the coordination of CO at high valent molybdenum sulfur centers, of special importance was $[Mo(CO)_2('^{bu}S_2')_2]$ (**4**) that carries no phosphine coligands which potentially stabilize metal CO bonds. **4** forms according to eqn. (7) when solid $[Mo(CO)_3('^{bu}S_4')]$ is kept at room temperature in high *vacuo* for 15 days.

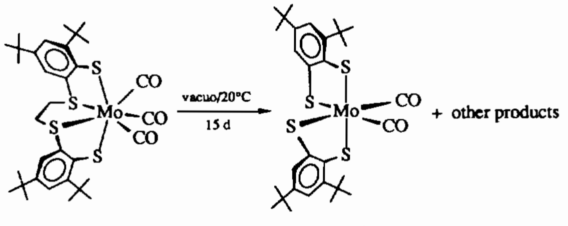

$[Mo(CO)_3('^{bu}S_4')]$ $[Mo(CO)_2('^{bu}S_2')_2]$ **4** (7)

Then, the orange–red $[Mo(CO)_3('^{bu}S_4')]$ slowly transforms into bright blue–violet **4**. **4** could be fully characterized by spectroscopy, is well soluble in all common organic solvents, and shows two sharp ν(CO) absorptions at very high frequencies in n-pentane (2041 and 2006 cm^{-1}; Fig. 2). The frequencies clearly indicate that the CO ligands are bound to molybdenum centers exhibiting low electron density and consequently high valent character.

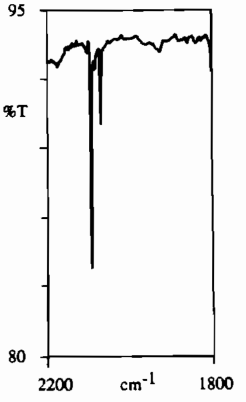

Fig. 2. ν(CO) IR spectrum of **4** in n-pentane.

4 is thermally less stable than the $[Mo(CO)(PR_3)('^{bu}S_2')_2]$ complexes. Therefore, it could not be synthesized in boiling THF, but it also formed in very small amounts by photolysis of $[Mo(CO)_3('^{bu}S_4')]$ according to eqn. (8).

$$[Mo(CO)_3)('^{bu}S_4')] \xrightarrow[h\nu]{CH_2Cl_2/-55\ °C} 4 + \text{other products} \qquad (8)$$

It is noted here that thioether desalkylations of this kind are equivalent to redox reactions because two neutral thioether S atoms transform into two uninegative thiolate S atoms.

X-ray structure analysis of $[Mo(CO)(PPh_3)('^{bu}S_2')_2]$ (1)

Single crystals were obtained of **1** such that a molybdenum(IV) carbonyl complex with a sulfur dominated coordination sphere could be characterized by X-ray structure analysis for the first time. Its molecular structure and the coordination geometry of the metal donor core of **1** are shown in Fig. 3. Table 3 lists selected distances and angles. See also 'Supplementary material'.

1 in solid state exhibits C_1 symmetry (Fig. 3(a)). The molybdenum center is surrounded in a nearly ideal pseudo trigonal prismatic manner by one C, one P and four S atoms (Fig. 3(b)). The mean deviations of the atoms from the tetragonal planes of the trigonal prism are only 2.0–6.7 pm. The '$^{bu}S_2$' ligands connect trigonal planes being practically parallel (dihedral angle 2.1°). The mean torsion angle of the trigonal planes of 3.4° is also very close to the limiting value of 0° in an ideal trigonal prism. The '$^{bu}S_2$' ligands coordinate the molybdenum center in such a way that C_2 symmetry results for the $[Mo('^{bu}S_2')_2]$ core.

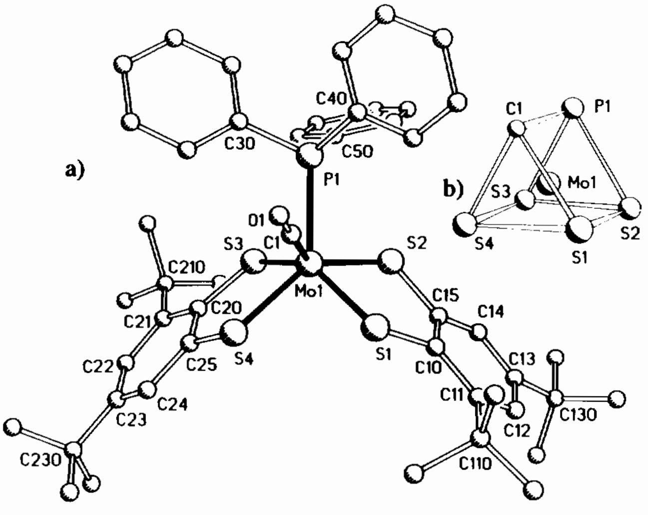

Fig. 3. (a) Molecular structure of **1** (H atoms omitted) and (b) pseudo trigonal prismatic geometry of the coordination skeleton.

TABLE 3. Selected distances (ppm) and angles (°) of **1**[a]

Distances		Angles	
Mo(1)–C(1)	204.2(6)	C(1)–Mo(1)–S(1)	79.0(2)
Mo(1)–S(1)	234.9(2)	C(1)–Mo(1)–S(2)	135.1(2)
Mo(1)–S(2)	235.8(2)	S(1)–Mo(1)–S(2)	81.4(1)
Mo(1)–S(3)	236.4(2)	C(1)–Mo(1)–S(3)	130.9(2)
Mo(1)–S(4)	235.0(2)	S(1)–Mo(1)–S(3)	142.5(1)
Mo(1)–P(1)	251.7(2)	S(2)–Mo(1)–S(3)	86.8(1)
C(1)–O(1)	113.4(7)	C(1)–Mo(1)–S(4)	79.8(2)
S(1)–C(10)	173.8(5)	S(1)–Mo(1)–S(4)	84.2(1)
S(2)–C(15)	173.6(6)	S(2)–Mo(1)–S(4)	137.5(1)
S(3)–C(20)	174.5(5)	S(3)–Mo(1)–S(4)	80.8(1)
S(4)–C(25)	172.9(6)	C(1)–Mo(1)–P(1)	82.3(2)
C(15)–C(14)	141.7(7)	S(1)–Mo(1)–P(1)	133.0(1)
C(15)–C(10)	141.3(8)	S(2)–Mo(1)–P(1)	82.2(1)
C(14)–C(13)	137.3(8)	S(3)–Mo(1)–P(1)	79.6(1)
C(13)–C(12)	140.4(9)	S(4)–Mo(1)–P(1)	133.9(1)
C(12)–C(11)	138.2(8)	Mo(1)–C(1)–O(1)	178.8(5)
C(11)–C(10)	143.4(8)	Mo(1)–S(1)–C(10)	110.5(2)
C(25)–C(24)	139.8(7)	Mo(1)–S(2)–C(15)	108.0(2)

[a]e.s.d.s are given in parentheses.

1 is structurally closely related to the trigonal prismatic molybdenum(VI) complex [Mo('S$_2$')$_3$] ('S$_2$'$^{2-}$ = 1,2-benzenedithiolate(2−)) [11]. The mean Mo–S (235.5 pm) and S–C distances (173.7 pm) in **1** do not significantly differ from those in [Mo('S$_2$')$_3$] (236.7 and 172.7 pm).

Trigonal prismatic coordination of molybdenum(IV) centers was also found in $[Mo\{S(CH_2CH_2S)_2\}_2]$ [12] and explained by discussing attractive interligand S···S interactions [13]. The formal substitution of thioether atoms by PhP groups leads to $[Mo\{PhP(CH_2CH_2S)_2\}_2]$ containing a pseudo octahedrally coordinated molybdenum(IV) center [13]. The different coordination geometries in both complexes were led back to the difference of five and three interligand S···S contacts that are possible in the $[MoS_6]$ and $[MoS_4P_2]$ cores of the respective complexes [13]. Only two interligand S···S contacts of similar size as in $[Mo\{S(CH_2CH_2S)_2\}_2]$ (295–339 pm) are found in **1** (315.1(3) and 324.5(3) pm). This demonstrates that stabilization of trigonal prismatic versus octahedral structures cannot be caused only by the number of possible interligand S···S contacts.

Discussion of distances observed in **1** is important with regard to the question whether it is justified to assign the oxidation state +IV to the molybdenum center. In fact, not only the high ν(CO) frequencies of [Mo(CO)(L)('^{bu}S$_2$')$_2$] (L = CO, PPh$_3$, PMe$_3$), but also the distances observed in **1** corroborate a high oxidation state of the molybdenum centers and exclude an oxidation of the benzenedithiolate ligands to dithiodiketone ligands according to eqn. (9).

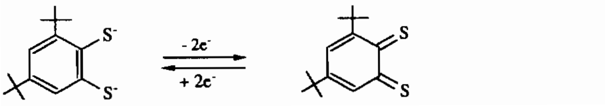

(9)

Such ligand centered redox steps are often discussed in redox reactions of dithiolene complexes with $S_2C_2R_2$ ligands, and argumentation heavily rests on increases and decreases of respective bond lengths [14, 15]. We analysed the relevant C–S and C–C distances in **1** and, for comparison, in closely related 'S$_4$' and '^{bu}S$_4$' complexes having metal centers in lower oxidation states, e.g. [Mo(NO)(NPMePh$_2$)('S$_4$')] [16], [μ-O{Mo(NO)('S$_4$')}$_2$] [17], [Mo(CO)$_2$(PMe$_3$)('S$_4$')] [16], [Mo(NO)(NH$_2$O)('S$_4$')] [18], [Mo(NO)$_2$('S$_4$')] [19] and [Fe(CO)$_2$('^{bu}S$_4$')] [20]. All C–S distances fall into the range 172.9(6)–176.2(6) pm and are so similar that it is impossible to assume shortened C–S bonds in **1**. Likewise the C–C distances within the aromatic rings of the sulfur ligands show no differences that could allow us to assume partial oxidation of the ligands. These experimental results correspond with calculations according to which 1,2-benzenedithiolate(2−) functions as a dianion even when coordinated to metal centers in high oxidation states [21], with results obtained with Fe^{IV} benzenedithiolato complexes [22], and finally also with the expectation that the benzene resonance energy should render difficult an oxidation according to eqn. (9) [15].

Consequently, the metal centers in [Mo(CO)(L)('^{bu}S$_2$')$_2$] complexes (L = CO, PPh$_3$, PMe$_3$) are to be regarded as Mo^{IV} centers. Then, however, they have 14e$^-$ configurations that have never been found in stable molybdenum carbonyl complexes before, cf. the similar situation in [Ru(S-2,3,5,6-Me$_4$C$_6$H)$_4$(CO)] [23], and the question is raised as to what the factors are that stabilize these electronically highly unsaturated metal centers. Comparison of the Mo–S distances in **1** and the complexes mentioned above yields the answer. The mean Mo–S distances are notably shorter in **1** (235.5 pm) than the mean Mo–S(thiolate) distances in, for example, [Mo(CO)$_2$(PMe$_3$)('S$_4$')] (250.6 pm) [16], [Mo(NO)(NH$_2$O)('S$_4$')] (247.8 pm) [18] or [Mo(NO)$_2$('S$_4$')] (245.1 pm) [19]. The short Mo–S distances in **1** indicate that the electron deficiency at the molybdenum center is reduced by S→Mo–π-donor bonds formed between occupied thiolate p orbitals and empty molybdenum d orbitals.

This explanation can be further supported by bond lengths found in [Mo(NO)(NPMePh$_2$)('S$_4$')] [16] and [μ-O{Mo(NO)('S$_4$')}$_2$] [17]. They formally contain electronically unsaturated Mo^{III} centers such that at least partial π-donation can be expected. Indeed, as it was previously found with Fe^{IV} benzenedithiolato complexes [22], these complexes exhibit metal thiolate distances of different length. The longer distances (249.2 and 248.3 pm) are equal to that in the molybdenum(II) complexes mentioned above, while the shorter ones (237.5 and 235.0 pm) compare with the Mo–S distances in **1**.

NMR spectra

^{1}H and ^{13}C{^{1}H} NMR spectra show that the structure of **1** in solution differs from that in solid state. The C_1 symmetry observed in solid state is expected to give rise to four tertiary butyl signals in the ^{1}H NMR spectrum, and in the ^{13}C{^{1}H} NMR spectrum to one CO doublet, four PPh$_3$ signals, and twelve signals of the aromatic and eight signals for the aliphatic C atoms of the '^{bu}S$_2$' ligands. But the ^{1}H (Fig. 4) and the ^{13}C{^{1}H} NMR spectra both display only half the number of the signals expected for the '^{bu}S$_2$' ligands indicating that **1** possesses not C_1 but twofold symmetry in solution. In a similar way, the number of ^{1}H and ^{13}C{^{1}H} NMR signals indicates that in **2**, **4** and **3** the '^{bu}S$_2$' ligands are symmetrically equivalent.

These observations are compatible with octahedral configurations of the complexes as shown in Fig. 5. In the case of [Mo(CO)(PR$_3$)('^{bu}S$_2$')$_2$] (R = Ph, Me) complexes, the NMR data correspond with the *trans* octahedral structures only (Fig. 5(a), (b)), while in the case of **4** and **3** *cis* octahedral structures (Fig. 5(c), (d)) also have to be considered. Conversions from trigonal prismatic to *trans* octahedral configurations require only relatively small deformations of angles and, therefore, the different structures of **1** in solid state and solution may be caused by crystal packing or solvent effects and need not have electronic reasons.

The PPh$_3$ ligand of **1** gives rise to two broad unresolved ^{1}H NMR signals centered at 7.3 and 6.7 ppm at room temperature (Fig. 6). Because this effect could have been due to hindered rotations of the phosphine ligand around the Mo–P axis, we recorded ^{1}H and ^{31}P{^{1}H} NMR spectra of **1**, **2** and **3** at variable temperature in order to gain more detailed information. Lability of the complexes (see above) made possible these measurements only at temperatures below 25 °C.

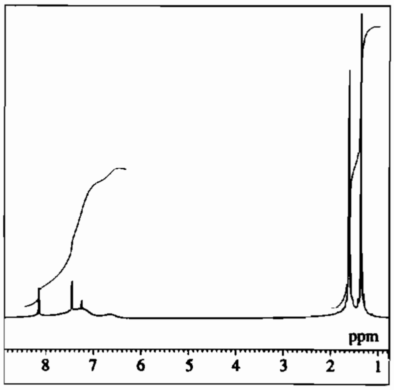

Fig. 4. ^{1}H NMR spectrum (270 MHz) of **1** in CDCl$_3$.

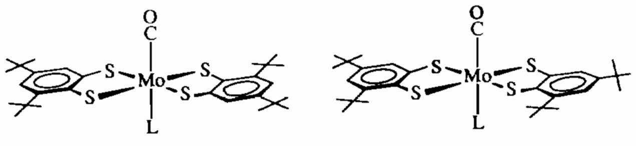

a) *trans* (C$_2$ or C$_{2h}$) b) *trans* (C$_s$ or C$_{2h}$)

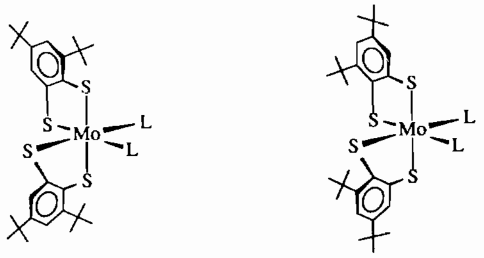

c) *cis* (C$_2$) d) *cis* (C$_2$)

Fig. 5. *trans* and *cis* octahedral structures of [Mo(CO)(L)('^{bu}S$_2$')$_2$] (L = CO, PPh$_3$, PMe$_3$) and [Mo(L)$_2$('^{bu}S$_2$')$_2$] (L = CO, PMe$_3$).

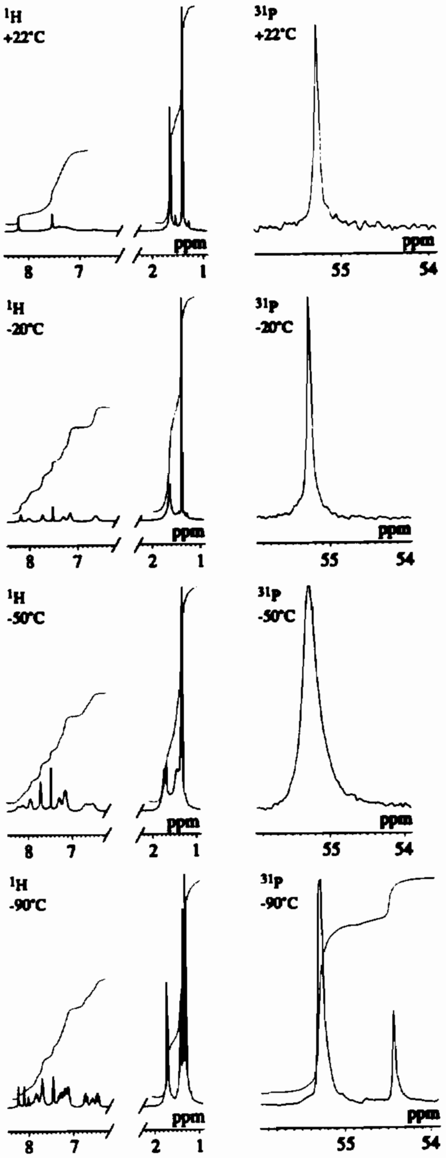

Fig. 6. ^{1}H and ^{31}P{^{1}H} NMR spectra of **1** in CD$_2$Cl$_2$ at variable temperature.

The NMR spectra obtained by cooling the probes down to −90 °C were unexpectedly complicated. In the case of the PPh_3 complex (Fig. 6) the broad PPh_3 signals split up into five separate signals at −20 °C and finally gave numerous sharp multiplets at −90 °C. One of the two tertiary butyl signals simultaneously changed, and the $^{31}P\{^1H\}$ singlet being sharp at 22 °C split up into at least two signals at −90 °C.

The NMR spectra of **2** and **3** were likewise temperature dependent. For instance, the ^{31}P signals being singlets at 22 °C each split up into three singlets at low temperatures.

The splitting of signals, in particular the rise of several ^{31}P signals, doubtlessly is caused by formation of several stereoisomers at low temperatures. They could be due to freezing of 'ring flipping' motions of the sulfur ligands, as suggested by Lazarowych and Morris when interpreting the low temperature $^{31}P\{^1H\}$ NMR spectra of $[Mo(PMePh_2)_2(\text{'}S_2\text{'})_2]$ [9], but as well to freezing of rotations that are largely unhindered at room temperature.

In the latter case, for instance in **1**, rotations of the PPh_3 ligand around the Mo–P axis, of PPh_3 phenyl rings around the P–C bonds, of tertiary butyl groups with respect to the aromatic ring, and of tertiary butyl methyl groups with respect to each other have to be taken into account. Because freezing of the individual rotations is to be expected to occur at different temperatures, this plausibly explains the emergence of very complex spectra at low temperatures.

Molecular models of octahedral *trans*-**1** furthermore indicate that the PPh_3 phenyl rings and the *ortho* tertiary butyl groups of the $\text{'}^{bu}S_2\text{'}$ ligands could influence each other. If this holds, then the splitting of both the ^{31}P and the tertiary butyl ^1H signals at −90 °C can be traced back to conformers that only differ in the position of the PPh_3 'propeller' with regard to the $[MoS_4]$ plane and, additionally, in the positions of the C_6H_5 rings with regard to themselves.

In our opinion, freezing of rotations plausibly explains the spectral changes at variable temperatures and is more probable than freezing of 'ring flipping' motions. Freezing of different rotations at different temperatures explains why the splitting of phosphine ^1H signals in all three complexes is more strongly temperature dependent than the splitting of $\text{'}^{bu}S_2\text{'}$ ^1H signals. If 'ring flipping' took place, the opposite behaviour would be expected.

Conclusions

$[Mo(CO)(L)(\text{'}^{bu}S_2\text{'})_2]$ with L = CO, PPh_3 and PMe_3 were synthesized, fully characterized, and identified as complexes containing high valent molybdenum sulfur centers that are capable of binding CO. Assignment of the oxidation state +IV to the molybdenum centers is based on the high ν(CO) absorptions and an analysis of the distances in $[Mo(CO)(PPh_3)(\text{'}^{bu}S_2\text{'})_2]$ (**1**) whose molecular structure was elucidated by X-ray structure determination. In particular, the short Mo–S distances indicate that electron deficiency at the molybdenum centers is reduced not by partial oxidation of the benzenedithiolate ligands but by $S \rightarrow Mo$–π-donor bonds.

NMR spectra show that **1** in solution possesses a molecular structure of twofold symmetry in contrast to the C_1 symmetry found in solid state. In a similar way, NMR spectra indicate symmetry equivalence of the $\text{'}^{bu}S_2\text{'}$ ligands in $[Mo(CO)(PMe_3)(\text{'}^{bu}S_2\text{'})_2]$ (**2**), $[Mo(CO)_2(\text{'}^{bu}S_2\text{'})_2]$ (**4**) and $[Mo(PMe_3)_2(\text{'}^{bu}S_2\text{'})_2]$ (**3**), and only correspond with *trans* or *cis* octahedral structures. The NMR spectra furthermore are dependent on temperature giving rise to very complex splitting patterns at low temperatures.

The function of molybdenum being found in the active sites of Fe/Mo nitrogenases is still open to question. Although never proved, molybdenum is usually assumed to be the binding site of N_2 as well as of the nitrogenase inhibitor CO, in spite of numerous results indicating the relatively high oxidation state of +IV for the sulfur coordinated molybdenum centers. In this context **4** and $[Mo(CO)(PR_3)(\text{'}^{bu}S_2\text{'})_2]$ (R = Ph, Me) complexes with their high valent molybdenum sulfur centers can be regarded as suitable model compounds. In fact, **4** is the first example showing that CO can bind to Mo^{IV} centers which exclusively exhibit biologically relevant thiolate donors.

Accordingly, do molybdenum centers of Fe/Mo nitrogenases have to be the binding site for the nitrogenase inhibitor CO as well as for the N_2 molecule? Even after the discovery of 'Fe-only' nitrogenases, this cannot be fully excluded. However, it may also be possible that N_2 binds to the iron centers and CO to the molybdenum centers. The primary consequence could be a hindrance of electron flow within the Fe/Mo cluster such that reduction of N_2 is prevented. Although it is bound, it does not get delivered electrons. Thus, the function of molybdenum in Fe/Mo nitrogenases is still open to question.

Supplementary material

Further details of the X-ray structure analysis of $[Mo(CO)(PPh_3)(\text{'}^{bu}S_2\text{'})_2]$ (**1**) have been deposited with the Fachinformationszentrum Karlsruhe GmbH, W-7514 Eggenstein-Leopoldshafen 2, FRG, and can be obtained by quoting deposition no. CSD 320252, the authors' names, and the reference.

Acknowledgements

We gratefully acknowledge support of these investigations by the Deutsche Forschungsgemeinschaft, the Bundesministerium für Forschung und Technologie, and the Fonds der Chemischen Industrie.

References

1 (a) D. Sellmann, H. Schillinger and F. Knoch, *Z. Naturforsch.*, in press; (b) D. Sellmann, F. Grasser, F. Knoch and M. Moll, *Angew. Chem., 103* (1991) 1346; *Angew. Chem., Int. Ed. Engl., 30* (1991) 1311.

2 F. J. Bergersen and J. R. Postgate (eds.), *A Century of Nitrogen Fixation Research,* The Royal Society, London, 1987.

3 J. R. Chrisnell, R. Premakumar and P. E. Bishop, *J. Bacteriol., 170* (1988) 27.

4 R. L. Richards, in A. Müller and W. E. Newton (eds.), *Nitrogen Fixation,* Plenum, New York, 1983, p. 275.

5 (a) B. K. Burgess, *Chem. Rev., 90* (1990) 1377; (b) G. N. Schrauzer, in W. E. Newton, J. R. Postgate and C. Rodriguez-Barrueco (eds.), *Recent Developments in Nitrogen Fixation,* Academic Press, London, 1977, p. 109; (c) R. W. F. Hardy, F. Bottomley and R. C. Burns (eds.), *A Treatise on Dinitrogen Fixation, Sections I and II: Inorganic and Physical Chemistry and Biochemistry,* Wiley, New York, 1979, p. 433.

6 (a) E. Roland, E. C. Walborsky, J. C. Dewan and R. R. Schrock, *J. Am. Chem. Soc., 107* (1985) 5795; (b) E. C. Walborsky, D. E. Wigley, E. Roland, J. C. Dewan and R. R. Schrock, *Inorg. Chem., 26* (1987) 1615; (c) M. Kamata, T. Yoshida and S. Otsuka, *J. Am. Chem. Soc., 103* (1981) 3011; (d) M. Kamata, K. Hirotsu, T. Higuchi, K. Tatsumi, R. Hoffman, T. Yoshida and S. Otsuka, *J. Am. Chem. Soc., 103* (1981) 5772.

7 J. A. Crayston, M. J. Almond, A. J. Downs, M. Poliakoff and J. J. Turner, *Inorg. Chem., 23* (1984) 3051.

8 (a) R. J. Haines, R. S. Nyholm and M. H. B. Stiddard, *J. Chem. Soc. A,* (1966) 1606; (b) M. L. H. Green and W. E. Lindsell, *J. Chem. Soc. A,* (1967) 686; (c) B. S. Erler, J. C. Dewan, S. J. Lippard and D. R. Tyler, *Inorg. Chem., 20* (1981) 2719.

9 N. J. Lazarowych and R. H. Morris, *Can. J. Chem., 68* (1990) 558.

10 D. Sellmann, F. Grasser and M. Moll, *J. Organomet. Chem., 415* (1991) 367.

11 M. Cowie and M. J. Bennett, *Inorg. Chem., 15* (1976) 1584.

12 J. Hyde, L. Magin and J. Zubieta, *J. Chem. Soc., Chem. Commun.,* (1980) 204.

13 P. J. Blower, J. R. Dilworth, G. J. Leigh, B. D. Neaves, F. B. Normanton, J. Hutchinson and J. A. Zubieta, *J. Chem. Soc., Dalton Trans.,* (1985) 2647.

14 R. E. Eisenberg, *Prog. Inorg. Chem., 12* (1970) 295.

15 U. T. Mueller-Westerhoff and B. Vance, in G. Wilkinson and R. D. Gillard (eds.), *Comprehensive Coordination Chemistry,* Vol. 2, Pergamon, Oxford, 1987, Ch. 16.5, p. 595.

16 D. Sellmann, J. Keller, M. Moll, C. F. Campana and M. Haase, *Inorg. Chim. Acta, 141* (1988) 243.

17 D. Sellmann, B. Seubert, F. Knoch and M. Moll, *Z. Anorg. Allg. Chem., 600* (1991) 95.

18 D. Sellmann, B. Seubert, M. Moll and F. Knoch, *Angew. Chem., 100* (1988) 1221; *Angew. Chem., Int. Ed. Engl., 27* (1988) 1164.

19 D. Sellmann, J. Keller, M. Moll, H. P. Beck and W. Milius, *Z. Naturforsch., Teil B, 41* (1986) 1551.

20 D. Sellmann, G. Freyberger, R. Eberlein, E. Böhlen, G. Huttner and L. Zsolnai, *J. Organomet. Chem., 323* (1987) 21.

21 S. Alvarez, R. Vicente and R. Hoffmann, *J. Am. Chem. Soc., 107* (1985) 6253.

22 D. Sellmann, M. Geck, F. Knoch, G. Ritter and J. Dengler, *J. Am. Chem. Soc., 113* (1991) 3819.

23 M. M. Millar, T. O'Sullivan, N. de Vries and S. A. Koch, *J. Am. Chem. Soc., 107* (1985) 3714.